

## A hard medium survey with ASCA

### IV. The radio-loud type 2 QSO AX J0843+2942

R. Della Ceca<sup>1</sup>, V. Braito<sup>1,2</sup>, V. Beckmann<sup>3</sup>, A. Caccianiga<sup>1</sup>, I. Cagnoni<sup>4</sup>, I. M. Gioia<sup>5</sup>, T. Maccacaro<sup>1</sup>,  
P. Severgnini<sup>1</sup>, and A. Wolter<sup>1</sup>

<sup>1</sup> Osservatorio Astronomico di Brera, via Brera 28, 20121 Milano, Italy  
e-mail: braito@brera.mi.astro.it; caccia@brera.mi.astro.it; tommaso@brera.mi.astro.it;  
paola@brera.mi.astro.it; anna@brera.mi.astro.it

<sup>2</sup> Dipartimento di Astronomia, Università degli Studi di Padova, vicolo dell'Osservatorio 2, 35122 Padova, Italy

<sup>3</sup> INTEGRAL Science Data Centre, Chemin d'Ecogia 16, 1290 Versoix, Switzerland  
e-mail: Volker.Beckmann@obs.unige.ch

<sup>4</sup> Dipartimento di Scienze, Università dell'Insubria, Como, Italy  
e-mail: ilaria.cagnoni@uninsubria.it

<sup>5</sup> Istituto di Radioastronomia CNR, via P Gobetti 101, 40129, Bologna, Italy  
e-mail: gioia@ira.cnr.it

Received 27 February 2003/ Accepted 16 May 2003

**Abstract.** We discuss the X-ray, optical and radio properties of AX J0843+2942, a high luminosity Type 2 AGN found in the ASCA Hard Serendipitous Survey. The X-ray spectrum is best described by an absorbed power-law model with a photon index of  $\Gamma = 1.72_{-0.6}^{+0.3}$  and intrinsic absorbing column density of  $N_{\text{H}} = 1.44_{-0.52}^{+0.33} \times 10^{23} \text{ cm}^{-2}$ . The intrinsic luminosity in the 0.5–10 keV energy band is  $\approx 3 \times 10^{45} \text{ erg s}^{-1}$ , well within the range of quasar luminosities. AX J0843+2942, positionally coincident with the core of a triple and strong ( $S_{1.4 \text{ GHz}} \sim 1 \text{ Jy}$ ;  $P_{1.4 \text{ GHz}} \sim 9 \times 10^{33} \text{ erg s}^{-1} \text{ Hz}^{-1}$ ) radio source, is spectroscopically identified with a Narrow Line object (intrinsic *FWHM* of all the permitted emission lines  $\lesssim 1200 \text{ km s}^{-1}$ ) at  $z = 0.398$ , having line features and ratios typical of Seyfert-2 like objects. The high X-ray luminosity, coupled with the high intrinsic absorption, the optical spectral properties and the radio power, allow us to propose AX J0843+2942 as a Radio-Loud “Type 2 QSO”. A discussion of the SED of this object is presented here together with a comparison with the SED of Ultra Luminous Infrared Galaxies, other “Type 2 QSO” candidates from the literature, and “normal” Radio-Quiet and Radio-Loud QSOs.

**Key words.** galaxies: active – quasars: individual: AX J0843+2942 – X-rays: galaxies – X-rays: individual: AX J0843+2942

### 1. Introduction

It is now largely accepted that X-ray obscured AGN play a significant (and perhaps major) role in the production of the Cosmic X-ray Background (CXB) above 2 keV (Comastri et al. 1995; Gilli et al. 2001). These objects should be the site where a large fraction of the energy density of the universe is generated (e.g. Fabian & Iwasawa 1999). In particular, the CXB synthesis models predict a large density of high luminosity ( $L_x > 10^{44} \text{ erg s}^{-1}$ ) X-ray obscured ( $N_{\text{H}} > 10^{22} \text{ cm}^{-2}$ ) AGN which, according to the Unified Model of AGN, should be characterized only by highly ionized narrow emission lines in the optical domain (the so called Type 2 QSO). Although doubts are often cast on the existence of “Type 2 QSO” (see e.g. Halpern et al. 1999; Akiyama et al. 2000), it is clear that hard X-ray surveys, which are less affected by the photoelectric absorption,

should provide a fundamental tool to detect and to study this elusive class of sources. In spite of these considerations, the number of high luminosity, X-ray obscured AGN in spectroscopically complete hard ( $E > 2 \text{ keV}$ ) X-ray selected samples is still very low. For instance there are no type 2 QSO amongst the 34 sources of the ASCA Large Sky Survey, which is a spectroscopically identified and complete sample selected in the 2–10 keV energy range (Akiyama et al. 2000). A few type 2 QSO “candidates” have been found using ASCA (Ohta et al. 1996; Akiyama et al. 2002) and ROSAT data (Almaini et al. 1995; Barcons et al. 1998; Barcons et al. 2003; Georgantopoulos et al. 1999). Some of them have been recently discovered in *Chandra* and XMM medium-deep surveys (Dawson et al. 2001; Crawford et al. 2002; Stern et al. 2002; Norman et al. 2002; Mainieri et al. 2002). Although these results seem to challenge the CXB synthesis model predictions, further X-ray spectroscopic investigations are needed.

Send offprint requests to: R. Della Ceca,  
e-mail: rdc@brera.mi.astro.it

**Table 1.** Basic information on AX J0843+2942.

ASCA seq.	RA; Dec (J2000) X RA; Dec (J2000) Opt.	Exp.(s) <i>S/N</i>	<i>HR1</i> <i>HR2</i>	Cts/s Optical ID
(1)	(2)	(3)	(4)	(5)
82011000	08 43 13; 29 42 46 08 43 10; 29 44 05	76 585 10.2	$0.85 \pm 0.10$ $0.14 \pm 0.07$	$(3.26 \pm 0.25) \times 10^3$ Type 2 QSOs at $z = 0.398$

Note – Columns are as follows: (1) ASCA sequence number; (2) source position as obtained from the centroid of the X-ray emission using the original astrometry from the ASCA GIS2 image and, second line, the position of the optical counterpart of the X-ray source from the POSS II image; (3) exposure time (GIS2 + GIS3) of the observation and, second line, source Signal-to-Noise ratio in the 2–10 keV energy range from the ASCA HSS catalog; (4) Hardness Ratio HR1 and, second line, HR2 obtained using the measured counts in the 0.7–2, 2–4 and 4–10 keV energy range (see Della Ceca et al. 1999); (5) net source count rate in the 0.9–10 keV energy band and, second line, identification of the optical counterpart. The source count rate represents about 66% of the total counts in the source extraction region.

According to the Unification Scheme of AGNs, a still unsettled fraction of the radiation emitted by the central engine is absorbed by the circumnuclear medium and re-emitted in the NIR/submillimeter bands. As a consequence, X-ray obscured AGN could also produce a significant fraction of the infrared background (Franceschini et al. 2002). In this respect it is worth noting that Type 2 QSO candidates have been also selected in the infrared domain amongst the ultra- and hyper-luminous infrared galaxies (e.g. IRAS 09104+4109, Franceschini et al. 2000; Iwasawa et al. 2001b). A detailed investigation of their Spectral Energy Distribution (SED) is thus mandatory to tackle many questions of the modern physical cosmology.

In this paper we discuss a Type 2 QSO, found in the ASCA Hard Serendipitous Survey (HSS, Cagnoni et al. 1998; Della Ceca et al. 1999; Della Ceca et al. 2000a,b), for which we have enough statistics to perform a broad band (1–10 keV) X-ray spectral analysis. The object discussed here is also a strong radio source and it could have been classified as a Narrow Line Radio Galaxy, a class of “potentially” obscured AGN (see Fabian et al. 2002; Derry et al. 2003 for X-ray observations of powerful radio galaxies) well known from radio surveys and which has been studied up to  $z = 5.19$  (van Breugel et al. 1999; see also McCarthy 1993 for a review). AX J0843+2942 is thus representative of the radio-loud tail of the type 2 quasar population.

The paper is organized as follows. In Sect. 2 we present the X-ray data and their analysis. In Sect. 3 we report the optical identification, as well as the X-ray, optical and radio properties of AX J0843+2942. Section 4 presents a discussion of the SED of AX J0843+2942 as well as the comparison with the SED of Ultra Luminous Infrared Galaxies, other “Type 2 QSOs”, and “normal” Radio-Quiet (RQ) and Radio-Loud (RL) QSOs from the literature. Finally, summary and conclusions are given in Sect. 5. We use  $H_0 = 50 \text{ km s}^{-1} \text{ Mpc}^{-1}$  and  $q_0 = 0$  throughout.

## 2. X-ray data and analysis

AX J0843+2942 was discovered during the optical identification process of the X-ray sources in the ASCA (2–10 keV energy range) HSS. The survey uses the data from the GIS2 instrument onboard ASCA (Tanaka et al. 1994). The source attracted our attention because of its position in the hardness ratio diagram (cf. Della Ceca et al. 1999) indicative of a hard

X-ray source. The data preparation for the X-ray spectral analysis was performed as in Della Ceca et al. (2000a) and is summarized below.

To maximize statistics and signal-to-noise ratio, total counts (source + background) were extracted from a circular region of 2' radius around the source centroid in the GIS2 and GIS3 images. Background counts were taken from two circular, source-free regions of 4.75' radius close to the source. GIS2 and GIS3 data, along with the relative background files and calibrations, were combined following the recipe given in the ASCA Data Reduction Guide<sup>1</sup>. The combined GIS spectrum was rebinned in order to have a signal-to-noise ratio greater than 3 in each energy channel; the energy interval with useful data is from  $\sim 0.9$  to 10 keV. Unfortunately, there are no ASCA SIS data associated to AX J0843+2942 since the source falls outside the SIS field of view. Spectral analysis has been performed using XSPEC 11.01. All the models discussed below have been filtered by the Galactic absorption column density along the line of sight ( $N_{\text{Hgal}} = 4.21 \times 10^{20} \text{ cm}^{-2}$ ; Hartmann & Burton 1997). Unless explicitly quoted, all the errors on the fitted spectral parameters represent the 68% confidence level for 1 interesting parameter ( $\Delta\chi^2 = 1.0$ ). Basic information for AX J0843+2942 is given in Table 1.

## 3. AX J0843+2942: A type 2 quasar candidate

### 3.1. X-ray spectrum

A single absorbed power-law model at the redshift of the optical counterpart ( $z = 0.398$ ; see Sect. 3.3) provides a good description of the ASCA spectrum of AX J0843+2942. The unfolded X-ray spectrum and the ratio between the data and the best fit model are shown in Fig. 1. No emission lines or absorption edges of statistical significance are found superimposed on the power law continuum. The 90% upper limit on the Fe  $K_\alpha$  line equivalent width at 6.4 keV (rest frame) is  $\sim 400$  eV; this upper limit is consistent with the Fe  $K_\alpha$  line equivalent width expected to be produced by transmission in the same medium which absorbs the continuum (cf. Lehly & Creighton 1993). Best fit spectral parameters, along with the observed fluxes and intrinsic luminosities in the (0.5–2) keV and (2–10) keV energy range, are reported in Table 2.

<sup>1</sup> see <http://heasarc.gsfc.nasa.gov/docs/asca/abc/abc.html>

**Table 2.** Results of the spectral fit (GIS2 + GIS3 data) for AX J0843+2942: absorbed power-law model at  $z = 0.398$ .

$\Gamma$	$N_{\text{H}}$	Flux	$L_x$	$\chi^2_{\nu}/\text{d.o.f.}$
	$10^{22} \text{ cm}^{-2}$	$10^{-13} \text{ erg cm}^{-2} \text{ s}^{-1}$	$10^{44} \text{ erg s}^{-1}$	
(1)	(2)	(3)	(4)	(5)
$1.72^{+0.3}_{-0.6}$	$14.4^{+3.3}_{-5.2}$	0.09; 14.2	10.7; 18.9	0.59/15

Note – Allowed ranges are at 68% confidence level for one interesting parameter ( $\Delta\chi^2 = 1.0$ ). Columns are as follows: (1) power-law photon index; (2) intrinsic absorbing column density; (3) observed flux (de-absorbed from the Galactic  $N_{\text{H}}$  value) in the 0.5–2 and 2–10 keV energy band; (4) intrinsic luminosity (i.e. the luminosity emitted from the nucleus) in the 0.5–2 and 2–10 keV energy band; (5) reduced  $\chi^2$  and degrees of freedom.

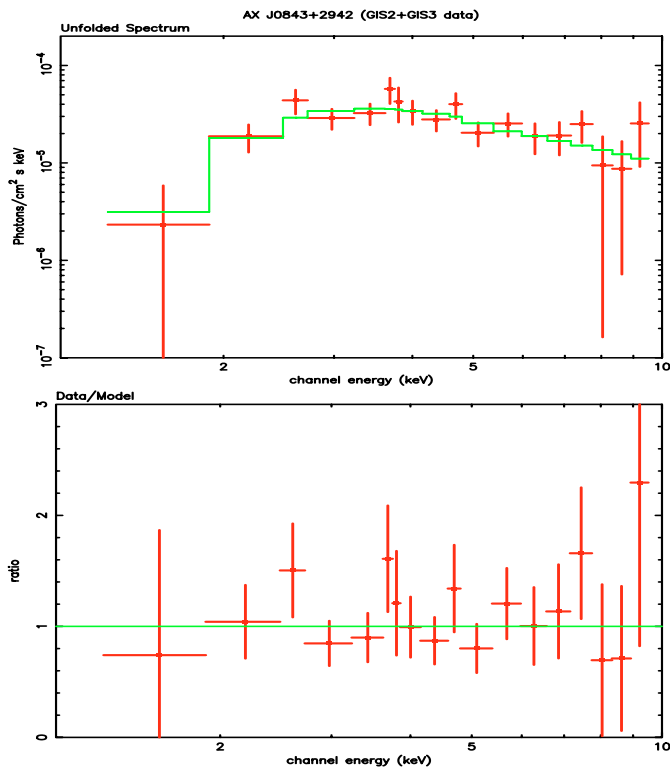


**Fig. 1.** AX J0843+2942: unfolded X-ray spectrum (upper panel) and the ratio between the data (GIS2+GIS3) and the best fit absorbed power-law model (lower panel).

In Fig. 2 we show the confidence contours for the photon index ( $\Gamma$ ) and the rest frame absorbing column density ( $N_{\text{H}}$ ). While  $\Gamma$  is not well constrained (the 90% confidence range is between 0.7 and 2.6), the best fit  $N_{\text{H}}$  is  $\approx 1.44 \times 10^{23} \text{ cm}^{-2}$ , with a 90% confidence range between  $6 \times 10^{22} \text{ cm}^{-2}$  and  $2.4 \times 10^{23} \text{ cm}^{-2}$ , and a 99% confidence level lower limit of  $4 \times 10^{22} \text{ cm}^{-2}$ . AX J0843+2942 is clearly an absorbed object; about 99.99% and 50% of the intrinsic rest-frame luminosity in the 0.5–2.0 keV and 2–10 keV energy band is absorbed. The intrinsic rest-frame luminosity ( $L_{(0.5-10) \text{ keV}} \approx 3 \times 10^{45} \text{ ergs s}^{-1}$  at  $z = 0.398$ , see Sect. 3.3) is well within the ‘‘High-Luminosity - QSO’’ regime. The combination of high luminosity, high intrinsic absorption and optical spectral properties (see Sect. 3.3) allow us to classify AX J0843+2942 as an X-ray obscured ‘‘Type 2 QSO’’.

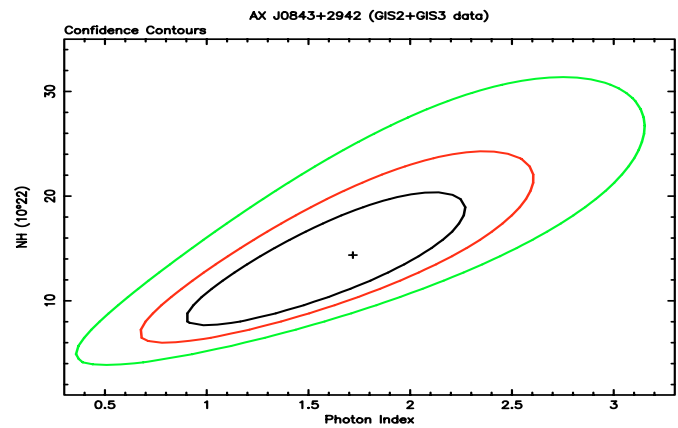


**Fig. 2.** Confidence contours (68%, 90% and 99% confidence level for two interesting parameters) for the photon index and the rest frame absorbing column density.

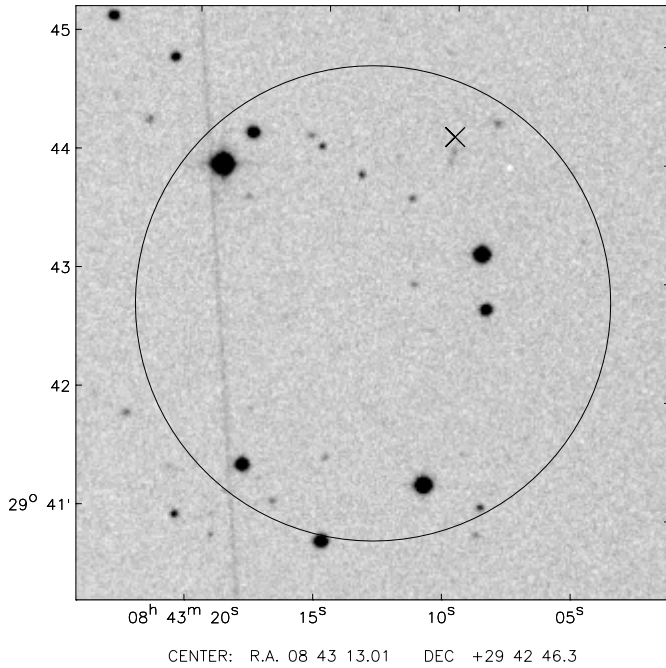
### 3.2. Source identification

Figure 3 shows the Palomar Observatory Sky Survey II (POSS II) image centered on the nominal X-ray position of AX J0843+2942 and its 90% error circle of  $2'$  radius. The cross marks the corrected X-ray position of AX J0843+2942, obtained by applying to the source the same offset measured for the target of the ASCA observation<sup>2</sup>.

In Fig. 4 we show the optical image centered at the corrected ASCA position (cross) with overlaid radio contours from the FIRST survey<sup>3</sup> (Becker et al. 1995; White et al. 1997). The brightest optical object close to the X-ray position is positionally coincident with the core of a triple radio source having a total flux density (1.4 GHz) of  $\sim 1 \text{ Jy}$ ; the properties of this radio source are discussed in Sect. 3.4. The probability to have a radio source with a flux  $\sim 1 \text{ Jy}$  inside a circle of  $2'$  radius is  $\sim 1.5 \times 10^{-4}$  (Condon et al. 1998), which implies 0.03 spurious coincidences among the 188 ASCA HSS sources. Therefore we conclude that the X-ray and the radio emission are very likely to be related and are both due to the same object, i.e. the object

<sup>2</sup> The target of this observation was MS0839.8+2938, an X-ray selected cluster of galaxies at  $z = 0.194$ . We have determined the sky position of the bulk of its X-ray emission using the ROSAT HRI observation rh800159. Unfortunately AX J0843+2942 is on the border of this ROSAT HRI observation (at about 16 arcmin offaxis) and is not detected.

<sup>3</sup> <http://sundog.stsci.edu/>



**Fig. 3.** POSS II image ( $5' \times 5'$ ) of the field centered at the “raw” X-ray position of AX J0843+2942. The circle represents the 90% confidence level error region of  $2'$  radius, while the cross marks the position of the X-ray centroid when the same offset measured for the target of the observation (MS0839.8+2938) is applied.

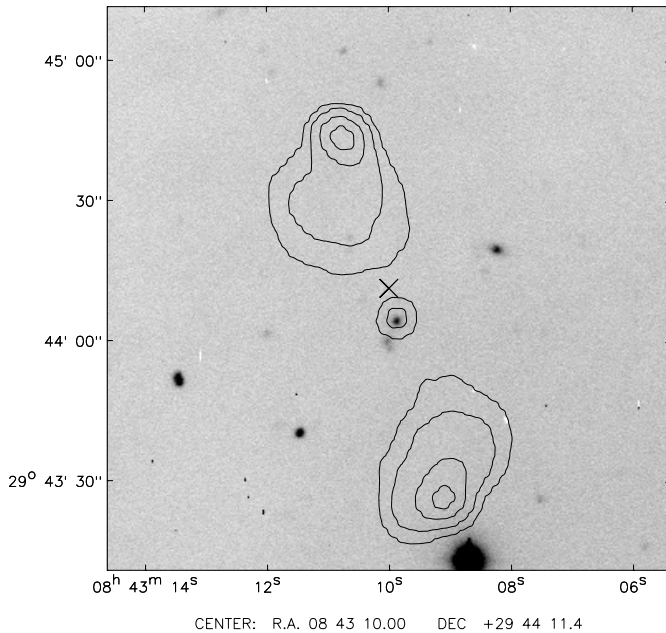


**Fig. 4.** CCD image ( $2' \times 2'$ ) centered at the revised ASCA position of AX J0843+2942 with overlaid radio contours (at 1, 3, 10,  $20\sigma$  above the background) from the FIRST radio survey.

positionally coincident with the core of the radio source (see Fig. 4). Optical, near infrared and far infrared photometry of this object are reported in Table 3.

### 3.3. Optical spectroscopy

The optical object coincident with the core of the radio source was observed spectroscopically at the  $88''$  telescope of the University of Hawaii on February 12th, 2000. Two 20-min exposures were taken using the Wide Field Grism Spectrograph (WFGS) equipped with the “blue” grism (400 grooves/mm) which gives a dispersion of  $4.1 \text{ \AA}/\text{pixel}$ .

The spectrum has been wavelength and flux calibrated using a Hg-Cd-Zn reference spectrum and the photometric standard SAO98781, respectively. No attempts have been made in order to have an absolute calibration of the final spectra. For the data reduction we have used the IRAF *longslit* package. The resulting spectrum, which is the sum of the two exposures, is presented in Fig. 5, while in Table 4 we report optical line properties.

The widths (*FWHM*) of the permitted lines are all below  $\sim 1200 \text{ km s}^{-1}$ , suggesting a spectroscopic classification of the object as a Narrow Emission Line object. The dominance of the  $[\text{OIII}]\lambda 5007$  when compared to the  $\text{H}\beta$  ( $[\text{OIII}]\lambda 5007/\text{H}\beta = 10$ ) excludes the classification as starburst or HII-region galaxy. The high  $[\text{OIII}]/\text{H}\beta$  ratio and the lack of evident Fe II lines exclude also the classification of AX J0843+2942 as Narrow Line Seyfert 1 (NLS1) whose optical spectrum are characterized by relatively weak forbidden lines ( $[\text{OIII}]\lambda 5007/\text{H}\beta < 3$ ) and strong Fe II multiplets (Osterbrock & Pogge 1985). The analysis of the  $\text{H}\beta$  profile does not reveal any strong evidence of a broad wing underlying the narrow component, although a better resolution spectrum is necessary to exclude completely the presence of a broad  $\text{H}\beta$  component.

In conclusion, AX J0843+2942 is optically classified as Seyfert 2-like object or, more appropriately, as an X-ray obscured type 2 QSO given its high X-ray luminosity and intrinsic absorption.

### 3.4. Radio properties

The radio counterpart of AX J0843+2942 is a triple radio source having the typical Fanaroff-Riley type II morphology, i.e. sharp edged lobes and bright hot spots (see Fig. 4). The absolute optical magnitude ( $M_E \simeq -21.5$ ) and the total radio power ( $\sim 9 \times 10^{33} \text{ ergs s}^{-1} \text{ Hz}^{-1}$ , see below) are consistent with the FR II classification according to the dividing line in the  $M - L_{\text{radio}}$  plane between FRI and FR II radio galaxies (Ghisellini & Celotti 2001 and references therein).

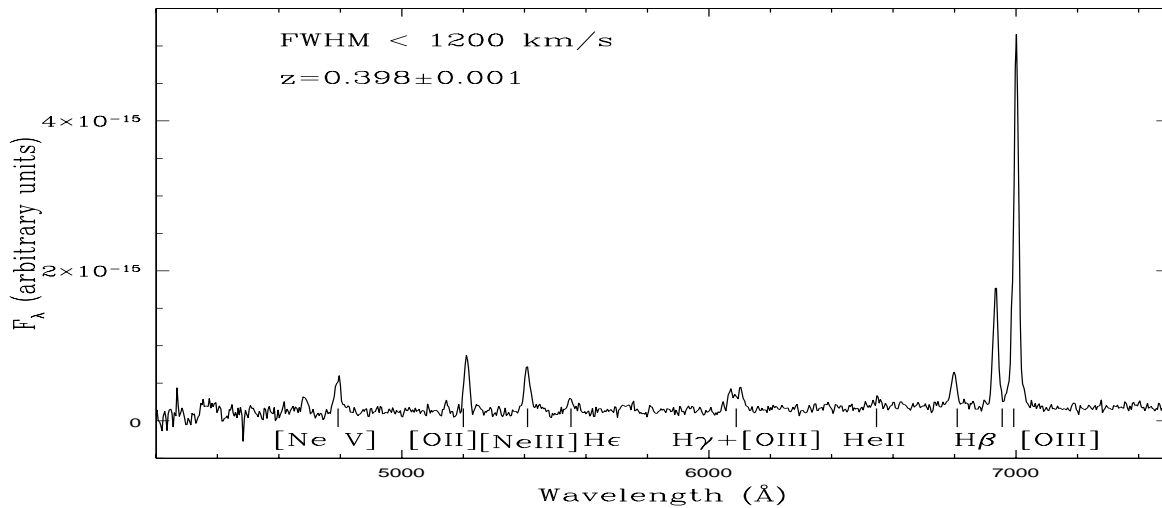
The total 1.4 GHz radio flux from the FIRST survey is  $878 \pm 44 \text{ mJy}$  corresponding to a radio power of  $(8.0 \pm 0.4) \times 10^{33} \text{ erg s}^{-1} \text{ z}^{-1}$  at the redshift of the source; the core flux density (power) is  $20.9 \pm 1.1 \text{ mJy}$  ( $P_{1.4 \text{ GHz}} = 0.19 \pm 0.01 \times 10^{33} \text{ erg s}^{-1} \text{ Hz}^{-1}$ ). The source is also detected in the lower spatial resolution NVSS survey<sup>4</sup> (Condon et al. 1998) as a double radio source. The total NVSS flux density (radio power) is  $986 \pm 40 \text{ mJy}$  ( $9.0 \pm 0.4 \times 10^{33} \text{ erg s}^{-1} \text{ Hz}^{-1}$ ). The radio flux density from the NVSS is a more reliable measure of the total flux since the VLA-B configuration used for the FIRST survey could miss some of the diffuse extended emission. This

<sup>4</sup> <http://info.cv.nrao.edu/~jcondon/nvss.html>

**Table 3.** Photometry of AX J0843+2942.

	Band	Frequency Hz	Observed flux density	$\nu f_\nu$ erg cm <sup>-2</sup> s <sup>-1</sup>	$\nu L_\nu$ erg s <sup>-1</sup>	Ref.
Radio	178 MHz	$1.78 \times 10^8$	4.7 Jy	$8.4 \times 10^{-15}$	$7.6 \times 10^{42}$	(1)
Radio (NVSS)	1.4 GHz	$1.4 \times 10^9$	985.7 mJy	$1.4 \times 10^{-14}$	$1.3 \times 10^{43}$	(2)
Radio	4.85 GHz	$4.85 \times 10^9$	354 mJy	$1.7 \times 10^{-14}$	$1.5 \times 10^{43}$	(3)
Far-Infrared (IRAS)	100 $\mu\text{m}$	$3.0 \times 10^{12}$	<0.8 Jy	$<2.4 \times 10^{-11}$	$<9.1 \times 10^{45}$	(4)
Far-Infrared (IRAS)	60 $\mu\text{m}$	$5.0 \times 10^{12}$	<0.3 Jy	$<1.5 \times 10^{-11}$	$<5.8 \times 10^{45}$	(4)
Far-Infrared (IRAS)	25 $\mu\text{m}$	$1.2 \times 10^{13}$	0.19 Jy	$2.3 \times 10^{-11}$	$8.7 \times 10^{45}$	(4)
Far-Infrared (IRAS)	12 $\mu\text{m}$	$2.5 \times 10^{13}$	<0.1 Jy	$<2.5 \times 10^{-11}$	$<9.5 \times 10^{45}$	(4)
Infrared (2MASS)	<i>K</i>	$1.36 \times 10^{14}$	15.3 mag	$6.9 \times 10^{-13}$	$2.6 \times 10^{44}$	(5)
Infrared (2MASS)	<i>H</i>	$1.82 \times 10^{14}$	>16.3 mag	$<5.8 \times 10^{-13}$	$<2.2 \times 10^{44}$	(5)
Infrared (2MASS)	<i>J</i>	$2.4 \times 10^{14}$	>16.5 mag	$<9.7 \times 10^{-13}$	$<3.7 \times 10^{44}$	(5)
Optical	<i>E</i>	$4.75 \times 10^{14}$	19.8 mag	$2.1 \times 10^{-13}$	$8.1 \times 10^{43}$	(6)
Optical	0	$7.4 \times 10^{14}$	21 mag	$8.2 \times 10^{-13}$	$3.2 \times 10^{43}$	(6)
X-ray (ASCA)	1.6 keV	$3.84 \times 10^{17}$	$5.16 \times 10^{-6}$ keV cm <sup>-2</sup> s <sup>-1</sup> keV <sup>-1</sup>	$1.3 \times 10^{-14}$	$1.3 \times 10^{43}$	(7)
X-ray (ASCA)	5.1 keV	$1.22 \times 10^{18}$	$1.3 \times 10^{-4}$ keV cm <sup>-2</sup> s <sup>-1</sup> keV <sup>-1</sup>	$1.1 \times 10^{-12}$	$1.1 \times 10^{45}$	(7)
X-ray (ASCA)	9.2 keV	$2.21 \times 10^{18}$	$1.0 \times 10^{-4}$ keV cm <sup>-2</sup> s <sup>-1</sup> keV <sup>-1</sup>	$1.5 \times 10^{-12}$	$1.5 \times 10^{45}$	(7)

Note: The quoted luminosities have been *K*-corrected assuming the observed spectral indices in the radio ( $\sim 0.78$ ), IR-optical ( $\sim -1.8$ ) and X-ray ( $\sim -1.16$ ) domain. References: (1) Pillington & Scott (1965); (2) total flux density from the NVSS survey (Condon et al. 1998); (3) Gregory & Condon (1991); (4) the upper limits derive from the IRAS Faint Source Catalog v2.0. The detection at 25  $\mu\text{m}$  is at  $S/N = 3$  and derives from the ADDSCAN processing of IRAS data; (5) from the 2MASS survey (see <http://www.ipac.caltech.edu/2mass/>); (6) from the APM catalogue and corrected for blending; (7) this work.

**Fig. 5.** Optical spectrum of AX J0843+2942 with the prominent emission features labeled.

radio source has been also detected at 178 MHz (4C +29.31, Pilkington & Scott 1965) and at 4.85 GHz (Gregory & Condon 1991). Assuming a power-law model the radio spectral index between 178 MHz and 4.85 GHz is  $\sim 0.78$ , consistent with the typical radio spectral index of lobe-dominated AGN. Total radio flux densities and powers are reported in Table 3. The projected separation of the two bright hot spots is  $\sim 80$  arcsec on sky, corresponding to a physical projected size of 0.57 Mpc at the redshift of the source; the ratio between the core flux and the total flux is about 0.021. Given the discussed radio

properties, the object is clearly a radio-loud and lobe-dominated AGN. In this respect we note that the measured size is comparable with the size of the known giant radio galaxies studied by Lara et al. (2001) and Schoenmakers et al. (2001).

#### 4. Discussion

It is interesting to compare the SED of AX J0843+2942 with the SED of other classes of AGNs to see if there are similarities and/or differences. In particular we are interested in the

**Table 4.** Optical line properties of AXJ0843+2942.

Line	Position (observed) Å	$z$	$EW$ (rest) Å	$FWHM$ km s <sup>-1</sup>
(1)	(2)	(3)	(4)	(5)
[NeV]	4792	0.3987	80	1400
[OII]	5211	0.3982	85	1050
[NeIII]	5408	0.3978	90	1300
H $\epsilon$	5549	0.3977	30	1200
H $\delta$	~5729	0.397:	~14	–
H $\gamma$ +[OIII]	~6070/6102	0.399:	~85	–
HeII	~6548	0.397:	~11	~1200
H $\beta$	6798	0.3985	30	850
[OIII]	6934	0.3983	90	750
[OIII]	7001	0.3982	300	750

comparison with the classes of AGNs where absorption effects can strongly modify their appearance and classification depending on the observational wavelength. Photometric data used to construct the SED of AX J0843+2942 have been summarized in Table 3.

Particular care must be taken on how to normalize the *observed* SEDs since many of the objects discussed below are either affected by heavy absorption (which modifies the intrinsic SEDs) or contaminated (and even dominated) by the possible starburst contribution, particularly in the infrared domain. Indeed there is now strong evidence that the processes of star-formation and AGN emission mostly happen in a high-density medium ( $N_H > 10^{23-24}$  cm<sup>-2</sup>), characterized by high dust extinction of the UV-optical flux and strong photoelectric absorption of the soft X-rays (see e.g. Levenson et al. 2001; Iwasawa 1999, and reference therein).

The first comparison (Fig. 6) is with three well known local AGN: the ultraluminous infrared galaxy (ULIRG hereafter) NGC 6240 ( $L_{\text{FIR}} \sim 5 \times 10^{45}$  ergs s<sup>-1</sup> at  $z = 0.0245$ ), the nearby far-infrared galaxy NGC 4945 ( $L_{\text{FIR}} \sim 3 \times 10^{44}$  ergs s<sup>-1</sup> at  $z = 0.00187$ ) and the powerful radio-galaxy Cygnus A ( $L_{\text{FIR}} \sim 2 \times 10^{45}$  ergs s<sup>-1</sup> at  $z = 0.0562$ ).

NGC 6240<sup>5</sup> and NGC 4945 have been classified as LINER and/or starburst galaxies on the basis of optical (Veilleux et al. 1995) and mid-/far-IR (Genzel et al. 1998) spectroscopy. For both objects, however, the *BeppoSAX* PDS observations at  $E > 10$  keV have clearly revealed the presence of a deeply buried AGN ( $N_H \approx \text{few} \times 10^{24}$  cm<sup>-2</sup>) with a QSO-like intrinsic luminosity in the case of NGC 6240 ( $L_{2-10 \text{ keV}} \sim 3.6 \times 10^{44}$  ergs s<sup>-1</sup>; Vignati et al. 1999) and a Seyfert-like luminosity in the case of NGC 4945 ( $L_{2-10 \text{ keV}} \sim 4 \times 10^{42}$  ergs s<sup>-1</sup>;

Guainazzi et al. 2000). Cygnus A is a nearby and powerful radio galaxy having a compact nucleus which is well described, in the X-ray domain, by an absorbed ( $\sim 2 \times 10^{23}$  cm<sup>-2</sup>) power law spectrum. Its unabsorbed luminosity ( $L_{(2-10 \text{ keV})} \sim 3.7 \times 10^{44}$  erg s<sup>-1</sup>) is in the QSOs range (Young et al. 2002).

The comparison of these three objects with AX J0843+2942 is shown in Fig. 6a (NGC 6240), in Fig. 6b (NGC 4945) and in Fig. 6c (Cygnus A). The SED of NGC 6240, NGC 4945 and Cygnus A have been tied to that of AX J0843+2942 under the hypothesis that the nuclear and intrinsic AGN emission emerges above  $\sim 20$  keV<sup>6</sup>.

The second comparison (shown in Figs. 7a, and 7b) is with the SED of distant type 1 and type 2 AGN. The SED of “normal” type 1 RL and RQ QSOs (labeled in Figs. 7a, 7b) are taken from Elvis et al. (1994). As for the distant type 2 QSOs we have used two objects for which enough photometric data are available to investigate their broad band properties over a large energy range ( $\sim 10$  decades in frequency) and a firm measure of the intrinsic AGN spectra above  $\sim 20$  keV is also available. The two objects are IRAS09104+4109 and AX J08494+4454.

IRAS09104+4109, the most luminous object in the  $z < 0.5$  Universe, is an ULIRG ( $L_{\text{IR}} \sim 2 \times 10^{46}$  erg s<sup>-1</sup>) at  $z = 0.442$ . *BeppoSAX* observations (Franceschini et al. 2000; see also Iwasawa et al. 2001b for the *Chandra* observation) have allowed the investigation of this source up to  $\sim 80$  keV, and have clearly revealed the presence of a deeply buried AGN. The absorbing column density towards the nucleus is  $\geq 5 \times 10^{24}$  cm<sup>-2</sup>

<sup>5</sup> A recent *Chandra* observation of NGC 6240 has revealed the presence of two active galactic nuclei of comparable luminosity in the core of this object (Komossa et al. 2003). In the following discussion we will consider the integrated emission from the two nuclei.

<sup>6</sup> It is worth noting that when a column density exceeds  $10^{24}$  cm<sup>-2</sup>, even the high-energy continuum (i.e., above the absorption cut-off) will be suppressed significantly by Compton down-scattering (see Matt et al. 1999). This is a geometry-dependent effect; the suppression is larger as the covering fraction of the absorber is smaller. Therefore the intrinsic power-law continuum could be somewhat higher (e.g., 20–50 per cent for  $N_H \approx 10^{24} - 5 \times 10^{24}$  cm<sup>-2</sup>) in the Compton-Thick objects, NGC 6240, NGC 4945, and IRAS 09104+4109 (see Fig. 7a for this latter object).

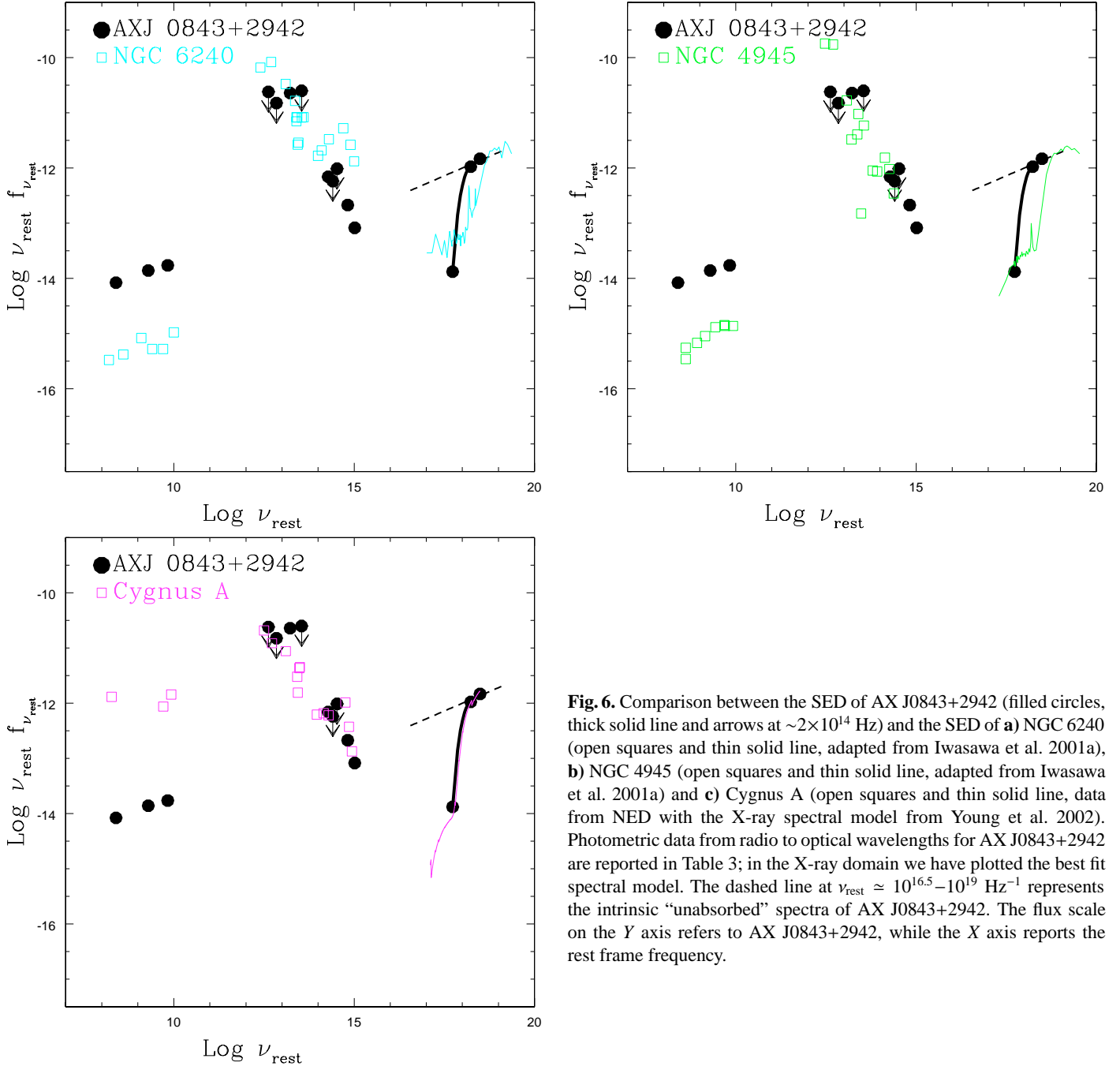


**Fig. 6.** Comparison between the SED of AX J0843+2942 (filled circles, thick solid line and arrows at  $\sim 2 \times 10^{14}$  Hz) and the SED of **a)** NGC 6240 (open squares and thin solid line, adapted from Iwasawa et al. 2001a), **b)** NGC 4945 (open squares and thin solid line, adapted from Iwasawa et al. 2001a) and **c)** Cygnus A (open squares and thin solid line, data from NED with the X-ray spectral model from Young et al. 2002). Photometric data from radio to optical wavelengths for AX J0843+2942 are reported in Table 3; in the X-ray domain we have plotted the best fit spectral model. The dashed line at  $\nu_{\text{rest}} \simeq 10^{16.5} - 10^{19}$  Hz $^{-1}$  represents the intrinsic “unabsorbed” spectra of AX J0843+2942. The flux scale on the Y axis refers to AX J0843+2942, while the X axis reports the rest frame frequency.

and the unabsorbed (2–10) keV X-ray luminosity is  $\sim 8 \times 10^{45}$  erg s $^{-1}$ , which is within the range of quasar luminosities.

AX J08494+4454 is a type 2 QSOs candidate at  $z = 0.9$  found in the course of the optical identification of ASCA deep surveys in the Lynx field (Ohta et al. 1996). The 0.5–10 keV *Chandra* spectrum is hard and is well described by a power law continuum absorbed by an hydrogen column density of  $\sim 2 \times 10^{23}$  cm $^{-2}$ ; the unabsorbed luminosity in the 2–10 keV energy range is  $\sim 7 \times 10^{44}$  ergs s $^{-1}$  (Akiyama et al. 2002). Recent deep Subaru/IRCS *J*-band spectroscopic observations seem to suggest the presence of a broad H $\alpha$  component at the bottom of the narrow H $\alpha$  emission line, implying that AX J08494+4454

could be a luminous cousin of Seyfert 1.9 objects (Akiyama et al. 2002).

The SED of Type 1 RL and RQ QSOs have been normalized to the intrinsic “unabsorbed” flux of AX J0843+2942 at  $\sim 2$  keV. The SED of IRAS09104+4109 and AX J08494+4454 have been tied to that of AX J0843+2942 under the hypothesis that their emission above  $\sim 20$  keV represents the intrinsic AGN emission.

As expected, both the local and the distant absorbed AGN in Figs. 6 and 7 lack the optical-UV bump which characterizes the “normal” Type 1 QSOs. However they show a very similar behavior in the optical-infrared regime despite their different

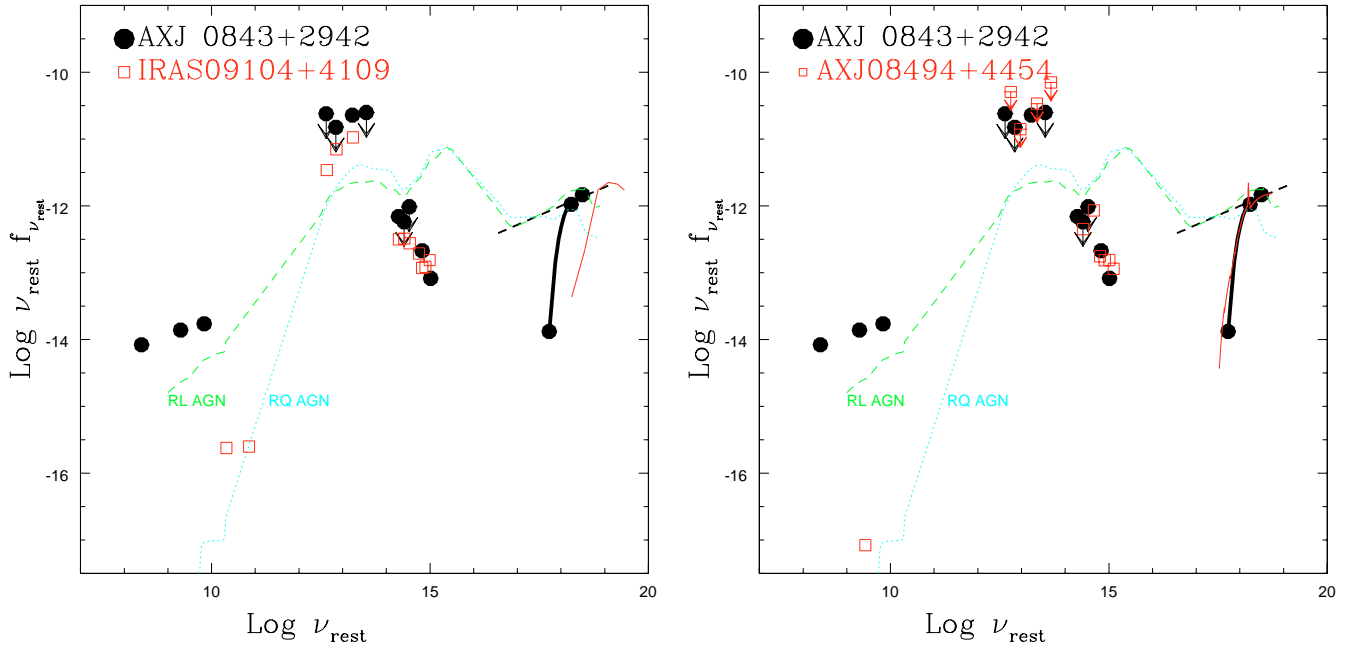


**Fig. 7.** Comparison between the SED of AX J0843+2942 (filled circles, thick solid line and arrows at  $\sim 2 \times 10^{14}$  Hz), the Type 1 RL and RQ QSOs (as labelled in the figure), the Type 2 QSOs IRAS09104+4109 (open squares and thin solid line) and the Type 2 QSOs AX J08494+4454 (open squares and thin solid line). The dashed line at  $\nu_{\text{rest}} \approx 10^{16.5} - 10^{19}$  Hz $^{-1}$  represents the intrinsic “unabsorbed” spectrum of AX J0843+2942. The SED of Type 1 RL and RQ QSOs have been adapted from Elvis et al. (1994); the SED of IRAS09104+4109 from Franceschini et al. (2000); and the SED of AX J08494+4454 from Akiyama et al. (2002) (and reference therein). The flux scale on the Y axis refers to AX J0843+2942, while the X axis refers to the rest frame frequency.

X-ray absorbing column density towards the nucleus (ranging from  $N_{\text{H}} \sim 2 \times 10^{23}$  to  $>5 \times 10^{24}$  cm $^{-2}$ ). The only object which deviates significantly is NGC 6240 in the optical and near-IR bands; for this object the optical near-IR photometric points were taken from NED and are usually measured with large apertures (K. Iwasawa, private communication). Two additional objects (CDF-S 202: a type 2 QSO at  $z = 3.7$  from Norman et al. 2002; and CXO52: a type 2 QSO at  $z = 3.288$  from Stern et al. 2002) show a similar behaviour although it is difficult to evaluate the real “intrinsic” spectrum given the poor X-ray statistics.

We tried to reproduce the near-infrared and optical colors of AX J0843+2942 assuming a “typical” QSO spectra template (continuum plus emission lines, adapted from Elvis et al. 1994 and Francis et al. 1991) and the extinction curve from Cardelli et al. (1989). A good description of the infrared-optical colors of AX J0843+2942 is obtained assuming  $E_{B-V} \sim 0.6$ . Provided that the X-ray and optical/NIR emission come from the same region (which may not be necessarily true), the implied  $E_{B-V}/N_{\text{H}}$  is  $\sim 4 \times 10^{-24}$  mag cm $^2$ , a factor about 40 less than the Galactic standard value of  $\sim 1.7 \times 10^{-22}$  mag cm $^2$  (Bohlin et al. 1978). This is a well known problem since the *Einstein* era (Maccararo et al. 1982) and has been recently discussed by Maiolino et al. (2001) in the context of different dust properties in the circumnuclear region of AGNs.

Finally under the simple assumptions used by Norman et al. (2002; e.g. the black hole is generating X-rays with an efficiency of  $\sim 1\%$  relative to the Eddington luminosity) we estimate a black hole mass of  $\sim 2 \times 10^9 M_{\odot}$ . This mass is similar to that measured in other steep spectrum radio quasars

having a similar total radio power of AX J0843+2942 (Lacy et al. 2001). By estimating the nuclear radiative output ( $L_{\text{ion}}$ ) using the well established relation between the luminosity in narrow emission lines (believed to result from the photoionization by the nuclear accreting radiation) and the radio power, we obtain (cf. Ghisellini & Celotti 2001)  $L_{\text{ion}} \sim 4 \times 10^{46}$  erg s $^{-1}$ . This value implies  $L_{\text{ion}}/L_{\text{EDD}} \sim 0.13$  and an accretion rate relative to the Eddington accretion rate of 1.3 (assuming an efficiency of 0.1). These values are consistent with the statement of Ghisellini & Celotti (2001) that, for the same black hole mass, the FR II radio-galaxies have a higher accretion rate if compared with FR I type objects.

## 5. Summary and conclusion

We have presented the X-ray, optical and radio properties of AX J0843+2942, a high luminosity Radio-Loud Type 2 AGN found in the ASCA Hard Serendipitous Survey. This source, positionally coincident with the core of a triple and strong ( $S_{1.4 \text{ GHz}} \sim 1$  Jy;  $P_{1.4 \text{ GHz}} \sim 9 \times 10^{33}$  erg s $^{-1}$  Hz $^{-1}$ ) radio source, is spectroscopically identified with a Narrow Line object (intrinsic *FWHM* of all the observed emission lines  $\lesssim 1200$  Km s $^{-1}$ ) at  $z = 0.398$ , with line features and ratios typical of Seyfert-2 like objects.

The X-ray spectrum is best described by an absorbed power-law model with photon index of  $\Gamma = 1.72_{-0.6}^{+0.3}$  and intrinsic absorbing column density of  $N_{\text{H}} = 1.44_{-0.52}^{+0.33} \times 10^{23}$  cm $^{-2}$  (99% confidence level lower limit of  $4 \times 10^{22}$  cm $^{-2}$ ). The intrinsic luminosity in the 0.5–10 keV energy band is  $\approx 3 \times 10^{45}$  erg s $^{-1}$ , well within the range of quasar luminosities.



The high X-ray luminosity, coupled with the high intrinsic absorption, optical spectral properties and radio power allow us to classify AX J0843+2942 as an X-ray obscured Radio-Loud “Type 2 QSO”.

We find strong similarities in the SED of AX J0843+2942 and the SED of local absorbed AGNs and distant Type 2 QSO in the optical near-infrared regime, despite the very different X-ray absorbing column densities towards the nucleus.

The near-infrared and optical colors of AX J0843+2942 can be reproduced assuming a “typical” QSO spectrum template and  $E_{B-V} \sim 0.6$ , implying an  $E_{B-V}/N_{\text{H}}$  that is a factor 40 less than the Galactic standard value.

The estimated black hole mass ( $\sim 2 \times 10^9 M_{\odot}$ ) is consistent with a relatively high accretion rate to power the bolometric luminosity of the QSO, in agreement with the dividing line between FRI and FRII type objects proposed by Ghisellini & Celotti (2001).

*Acknowledgements.* We thank K. Iwasawa, M. Akiyama and A. Franceschini for providing the data, shown in Figs. 6 and 7, in a tabular form. This work received partial financial support from the Italian Ministry for University and Research (MURST) and from ASI (I/R/037/01). K. Iwasawa is also thanked for useful comments in the referee report. This research has made use of the NASA/IPAC extragalactic database (NED), which is operated by the Jet Propulsion Laboratory, Caltech, under contract with the National Aeronautics and Space Administration. We thank all the members of the ASCA team who maintains the software data analysis and the archive.

## References

- Almaini, O., Boyle, B. J., Griffiths, R. E., et al. 1995, *MNRAS*, 277, L31
- Akiyama, M., Ohta, K., Yamada, T., et al. 2000, *ApJ*, 532, 700
- Akiyama, M., Ueda, Y., & Ohta, K. 2002, *ApJ*, 567, 42
- Barcons, X., Carballo, R., Ceballos, M. T., Warwick, R. S., & Gonzalez-Serrano, J. I. 1998, *MNRAS*, 301, L25
- Barcons, X., Carballo, R., Carrera, F. J., et al. 2003, *MNRAS*, in press [astro-ph/0303530]
- Becker, R. H., White, R. L., & Helfand, D. J. 1995, *ApJ*, 450, 559
- Bohlin, R. C., Savage, B. D., & Drake, J. F. 1978, *ApJ*, 224, 132
- Cagnoni, I., Della Ceca, R., & Maccacaro, T. 1998, *ApJ*, 493, 54
- Cardelli, J. A., Clayton, G. C., & Mathis, J. S. 1989, *ApJ*, 345, 245
- Condon, J. J., Cotton, W. D., Greisen, E. W., et al. 1998, *AJ*, 115, 1693
- Comastri, A., Setti, G., Zamorani, G., & Hasinger, G. 1995, *A&A*, 296, 1
- Crawford, C. S., Gandhi, P., Fabian, A. C., et al. 2002, *MNRAS*, 333, 809
- Dawson, S., Stern, D., Bunker, A. J., Spinrad, H., & Dey, A. 2001, *AJ*, 122, 598
- Della Ceca, R., Castelli, G., Braito, V., et al. 1999, *ApJ*, 524, 674
- Della Ceca, R., Maccacaro, T., Rosati, P., & Braito, V. 2000a, *A&A*, 355, 121
- Della Ceca, R., Braito, V., Cagnoni, I., & Maccacaro, T. 2000b, *Mem. SAIt.*, in press [astro-ph/0007430]
- Derry, P. M., O’Brien, P. T., Revees, J. N., et al. 2003, *MNRAS*, in press [astro-ph/0304550]
- Elvis, M., Wilkes, B. J., McDowell, J. C., et al. 1994, *ApJS*, 95, 1
- Fabian, A. C., & Iwasawa, K. 1999, *MNRAS*, 303, L34
- Fabian, A. C., Crawford, C. S., & Iwasawa, K. 2002, *MNRAS*, 331, L57
- Franceschini, A., Bassani, L., Cappi, M., et al. 2000, *A&A*, 353, 910
- Franceschini, A., Braito, V., & Fadda, D. 2002, *MNRAS*, 335, L51
- Francis, P. J., Hewett, P. C., Foltz, C. B., et al. 1991, *ApJ*, 373, 465
- Genzel, R., Lutz, D., Sturm, E., et al. 1998, *ApJ*, 498, 579
- Georgantopoulos, I., Almaini, O., Shanks, T., et al. 1999, *MNRAS*, 305, 125
- Gilli, R., Salvati, M., & Hasinger, G. 2001, *A&A*, 366, 407
- Ghisellini, G., & Celotti, A. 2001, *A&A*, 379, L1
- Gregory, P. C., & Condon, J. J. 1991, *ApJS*, 75, 1011
- Guainazzi, M., Matt, G., Brandt, W. N., et al. 2000, *A&A*, 356, 463
- Halpern, J. P., Turner, T. J., & George, I. M. 1999, *MNRAS*, 307, L47
- Hartmann, D., & Burton, W. B. 1997, *Atlas of Galactic Neutral Hydrogen* (Cambridge, New York: Cambridge University Press)
- Iwasawa, K. 1999, *MNRAS*, 302, 96
- Iwasawa, K., Matt, G., Guainazzi, M., & Fabian, A. C. 2001a, *MNRAS*, 326, 894
- Iwasawa, K., Fabian, A. C., & Etori, S. 2001b, *MNRAS*, 321, L15
- Komossa, S., Burwitz, V., Hasinger, G., et al. 2003, *ApJ*, 582, L15
- Lacy, M., Laurent-Muehleisen, S. A., Ridgway, S. E., Becker, R. H., & White, R. L. 2001, *ApJ*, 551, L17
- Lara, L., Márquez, I., Cotton, W. D., et al. 2001, *A&A*, 378, 826
- Leahy, D. A., & Creighton, J. 1993, *MNRAS*, 263, 314
- Levenson, N. A., Weaver, K. A., & Heckman, T. M. 2001, *ApJ*, 550, 230
- Maccacaro, T., Perola, G. C., & Elvis, M. 1982, *ApJ*, 257, 47
- Mainieri, V., Bergeron, J., Hasinger, G., et al. 2002, *A&A*, 393, 425
- Maiolino, R., Marconi, A., Salvati, M., et al. 2001, *A&A*, 365, 28
- Matt, G., Pompilio, F., & La Franca, F. 1999, *New Astron.*, 4, 191
- McCarthy, P. J. 1993, *ARA&A*, 31, 639
- Norman, C., Hasinger, G., Giacconi, R., et al. 2002, *ApJ*, 571, 218
- Ohta, K., Yamada, T., Nakanishi, K., et al. 1996, *ApJ*, 458, L57
- Osterbrock, D. E., & Pogge, R. W. 1985, *ApJ*, 297, 166
- Pilkington, J. D. H., & Scott, P. F. 1965, *MNRAS*, 69, 183
- Schoenmakers, A. P., de Bruyn, A. G., Röttgering, H. J. A., & van der Laan, H. 2001, *A&A*, 374, 861
- Stern, D., Moran, E. C., Coil, A. L., et al. 2002, *ApJ*, 568, 71
- Tanaka, Y., Inoue, H., & Holt, S. S. 1994, *PASJ*, 46, L37
- van Breugel, W., De Breuck, C., Stanford, S. A., et al. 1999, *ApJ*, 518, L61
- Veilleux, S., Kim, D.-C., Sanders, D. B., Mazzarella, J. M., & Soifer, B. T. 1995, *ApJS*, 98, 171
- Vignati, P., Molendi, S., Matt, G., et al. 1999, *A&A*, 349, L57
- White, R. I., Becker, R. H., Helfand, D. J., & Gregg, M. D. 1997, *ApJ*, 475, 479
- Young, A. J., Wilson, A. S., Terashima, Y., Arnaud, K. A., & Smith, D. A. 2002, *ApJ*, 564, 176